Thermofluidynamic Modelling of Hydrogen Absorption and Desorption in a $LaNi_{4.8}Al_{0.2}$ Hydride Bed

D. Baldissin*[1] and D. Lombardo*[1]
[1]Compumat S.r.l., via Quarello 11/A 10135 Torino (Italy)
*Corresponding author: daniele.baldissin@compumat.it, daniele.lombardo@compumat.it

Abstract: A two-dimensional mathematical model for the absorption and desorption of H_2 in $LaNi_{4.8}Al_{0.2}$ was developed and experimentally validated. The model is composed of an energy balance, a mass balance and a momentum balance. These differential equations are numerically solved by means of the finite element method using the software COMSOL Multyphysics™.
From a comparison between theoretical results and experimental data was found that an essential aspect of hydrogen storage in metal hydrides is related to the thermal characteristics of the reactor used, especially the properties of heat exchange: the overall heat transfer coefficient *h* and effective thermal conductivity k_{eff}.

Keywords: Hydrogen Storage, Heat and Mass Transfer, Modeling, Metal Hydrides

1. Introduction

Depletion of fossil fuel resources has led to significant research on alternative and cleaner fuels. Hydrogen energy seems to be the best alternative to fossil fuels due to its high calorific value and it already has several industrial applications in refrigerators, heat storage, compressors, heat engines and automotive industries. Hydrogen is also interesting because it produces more energy per unit weight than any other fuel.

However, storage problem of hydrogen prevents its wide usage and commercialization: low density of hydrogen exposes several storage problems such as high pressure and large volume requirements. Storing hydrogen in metal-hydride compounds appears to be the method of hydrogen storage of the future and therefore it has received much care in the scientific community. The application of this methodology requires the knowledge of the heat and mass transfer in a metal-hydrogen reactor during the absorption and desorption of hydrogen.

Many mathematical models for the description of hydrogen storage into metal hydrides are available in the literature [1-6]. Neverthless, most of them regards absorption processes. In this paper both absorption and desorption of hydrogen in metallic hydrides are taken into account.

The solution of partial differential equations (PDE) was performed using the COMSOL Multiphysics™ software. The aim of these simulations is to find out the best parameters for the heat exchange between the storage system and the external environment.

2. Use of COMSOL Multiphysics

Partial differential equations are numerically solved with FEM technique by using the COMSOL Multiphysics 3.3 software. The geometry used in modelling reactor 1 represents a longitudinal section with two subdomains: one for the porous media and one for the free space (figure 1).

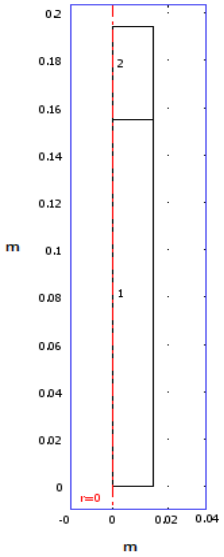

Figure 1. Geometry used in modelling reactor 1 (subdomain 1: porous media, subdomain 2: free space).

The mesh used has 292 points and 500 triangular element, leading to 3249 degrees of freedom.

The reactor 2 was modelled by using symmetry properties; therefore only one sector of the vessel section has been considered (figure 2). The mesh used for reactor 2 has 1040 points and 1977 triangular element, leading to 7810 degree of freedom. For both reactors a direct linear system solver has been used (UMFPACK), solving general PDEs in the interval 0:600 s, with time step of 1 s.

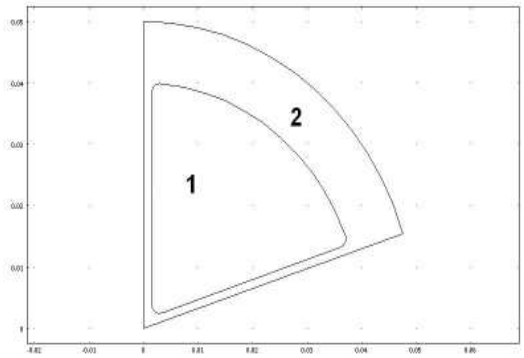

Figure 2. Geometry used in modelling the reactor 2 (subdomain 1: porous media, subdomain 2: steel wall).

3. Numerical Model

The simulated reactor consists of a cylindrical container that exchanges heat through the surfaces (bottom and sides). The vessel is filled with a powder of $LaNi_{4.8}Al_{0.2}$.

A free space is left to take into account of $LaNi_{4.8}Al_{0.2}$ expansion after the absorption of hydrogen gas (~ 20% of the total volume [1]).

The model was applied to two different cylindrical geometries without and with metal fins (geometry 1 and 2 respectively). Firstly, the theoretical model was validated by comparing the results of the calculation performed on the reactor 1 with experimental data; secondly the model has been applied to reactor 2 to study the effect of the fin insertion.

In order to simplify the problem the following assumptions were considered [2-4]:

a) local thermal equilibrium (LTE): gas and solid temperature is the same;
b) hydrogen is treated as ideal gas;
c) the effect of the H_2 concentration on the variation of equilibrium pressure is negligible (Van't Hoff equation);
d) the heat transfer by radiation is neglected.

3.1. Governing Equations

The proposed model consists of differential equations for the system (energy, mass and momentum balance) and equations that describe the kinetics of absorption and desorption [2-4].

Energy balance

Assuming thermal equilibrium between hydride powder and hydrogen, a single energy equation is solved instead of separate equations for both solid and gaseous phases:

$$\left(\rho C_p\right)_e \frac{\partial T}{\partial t} + \left(\rho_g C_{p_g}\right)\mathbf{v}_g \cdot \nabla T = \\ = \nabla \cdot \left(k_e \nabla T\right) + m\left(\Delta H - T\left(C_{pg} - C_{ps}\right)\right) \quad (1)$$

Considering only parallel heat conduction in solid and gas phases, the following expression for effective specific heat and thermal conductivity can be written:

$$\left(\rho C_p\right)_e = \left(\varepsilon \rho_g C_{p_g} + \left(1-\varepsilon\right)\rho_s C_{p_s}\right) \quad (2)$$

$$k_e = \varepsilon k_g + \left(1-\varepsilon\right)k_s \quad (3)$$

Equation (3) is substituted by using a value of k_e obtained by minimizing the error between the results of our calculation and the experimental data. (see also paragraph 5.3).

Hydride mass balance

For the solid a mass conservation equation is considered:

$$\left(1-\varepsilon\right)\frac{\partial\left(\rho_s\right)}{\partial t} = -m \quad (4)$$

Momentum balance

The following expression for momentum balance is used:

$$\frac{\partial \varepsilon \rho_g}{\partial t} + \nabla \cdot \left(\rho_g \mathbf{v}_g\right) = -m \quad (5)$$

Velocity of gas is obtained by the Darcy's law:

$$\mathbf{v}_g = -\frac{K}{\mu_g}\vec{\nabla}\left(p_g\right) \quad (6)$$

where K is the permeability of solid and μ_g the dynamic viscosity of the gas.

The source term m in equations (1), (4) and (5) for subdomain 2 is zero.

Kinetic expressions
The following kinetic expression for absorption (5) and desorption (6) are used [6]:

$$m = C_a \exp\left(-\frac{E_a}{R_g T}\right) \ln\left(\frac{p_g}{p_{eq}}\right)(\rho_{ss} - \rho_s) \qquad (7)$$

$$m = C_d \exp\left(-\frac{E_d}{R_g T}\right)\left(\frac{p_g - p_{eq}}{p_{eq}}\right)(\rho_s - \rho_0) \qquad (8)$$

where C is the pre-exponential constant, E the activation energy, ρ_{ss} the density of metal hydride at the saturation state and ρ_0 the initial metal hydride density

Moreover the following costitutive equations have been used.

Perfect gas law:

$$\rho_g = \frac{p_g \cdot M_{H_2}}{R_g T} \qquad (9)$$

in which M_{H2} is the molecular weight of hydrogen and R_g is the universal gas constant.

Van't Hoff law:

$$\ln p_{eq} = \frac{\Delta H}{R_g T} - \frac{\Delta S}{R_g} \qquad (10)$$

in which p_{eq} is the equilibrium pressure of hydrogen.

3.2. Initial and boundary conditions

Initially, gas and solid are at the same temperature. Pressure and hydride density are assumed to be costant:

$$T_s = T_g = T_0 \quad P_g = P_0 \quad \rho_s = \rho_0$$

Taking into account the simmetry of the reactor, the following conditions can be imposed along the z-axys:

$$\frac{\partial P}{\partial r}(z,0) = 0 \quad \frac{\partial T}{\partial r}(z,0) = 0$$

Tab 1. Parameters used in the model

Parameter	Symbol	Value
Initial temperature		
absorption	T_0	294 K
desorption		300 K
Initial pressure		
absorption	p_0	19 bar
desorption		2 bar
Initial hydride density	ρ_0	8300 kg m^{-3} [5]
Saturation hydride density	ρ_{ss}	8354 kg m^{-3} [5]
Hydride molecular weight	M_s	$426 \cdot 10^{-3}$ kg mol^{-1}
Gas molecular weight	M_g	$2 \cdot 10^{-3}$ kg mol^{-1}
Hydride specific heat	C_{ps}	355 J kg^{-1} K^{-1} [7]
Gas specific heat	C_{pg}	14890 J kg^{-1} K^{-1} [8]
Hydride porosity	ε	0.5
Reaction enthalpy	ΔH	-32600 J mol^{-1} [9]
Reaction entropy	ΔS	-104.5 J mol^{-1} K^{-1} [9]
Kinetic constant		
absorption	C_a	59.187 s^{-1} [3]
desorption	C_d	9.57 s^{-1} [4]
Activation energy		
absorption	E_a	21179.6 J mol^{-1} [3]
desorption	E_d	16420 J mol^{-1} [4]

The boundary conditions on the wall are set as follows [2-5]:

$$\frac{\partial P}{\partial r}(z,r) = 0 \quad \frac{\partial P}{\partial z}(z,r) = 0$$

Through the wall the following heat flux condition is set [2-5]:

$$-\mathbf{n} \cdot k_e \nabla T = h(T - T_f)$$

The overall heat transfer coefficient h was obtained by minimizing the error between the results of our calculation and the experimental data (see also paragraph 5.3) such as k_e.
On the other boundaries insulation or symmetry conditions have been used.

4. Experimental

The experimental apparatus consists of a metallic container with stainless steels walls, filled with a metallic powder of $LaNi_{4.8}Al_{0.2}$. It is

collocated into a water bath in order to keep constant temperature conditions. A source of H_2 is connected via a valve to the reactor and it is set at a constant pressure. During absorption, when the valve is opened, the gas enters the reactor and flows through the porous metallic powder (strong exothermic reaction). Two series of three thermocouples (K-type) are located inside the vessel to register the temperature behaviour. (figure 3).

Figure 3. Experimental apparatus: reactor into the water bath.

5. Results

5.1. Reactor 1

The main input data used for simulations are reported in Tab. 1. The numerical results for an internal point of the subdomain 1 are shown in the figures 4-7.

Temperature results are compared with experimental data. During hydrogen absorption the temperature of the vessel increases until to reach about 26 °C, due to an exothermic process; then it decreases until to the equilibrium temperature corrisponding to the bath's one (figure 4).

In figure 5 the behavior of the internal pressure is shown, from the initial value of 19 bar to the equilibrium pressure of 2 bar at the end of the absorption process.

During hydrogen desorption (figure 6), the temperature increases slowly within the vessel, due to endothermic reaction. After a period of time, the dehydriding reaction ends and the heat transfer problem occurs only by means of conduction. Finally external fluid temperature is reached.

Figure 7 shows the pressure behaviour inside the vessel: it increases from an initial value of 2 bar until to the reaching of the equilibrium pressure of 3.2 bar.

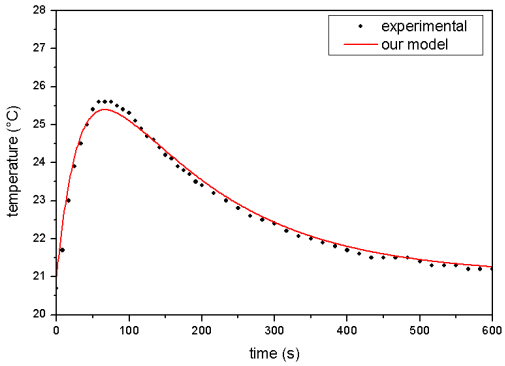

Figure 4. Temperature behavior in the vessel 1 during absorption: comparison between model results and experimental data.

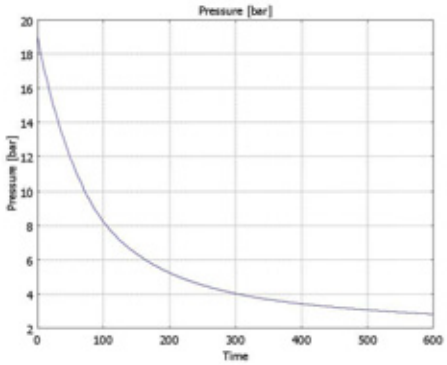

Figure 5. Internal pressure behavior during absorption

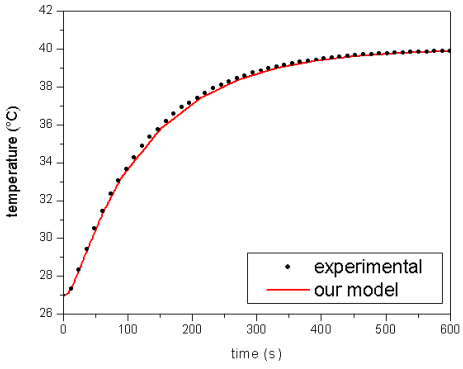

Figure 6. Temperature behavior in the vessel 1 during desorption: comparison between model results and experimental data.

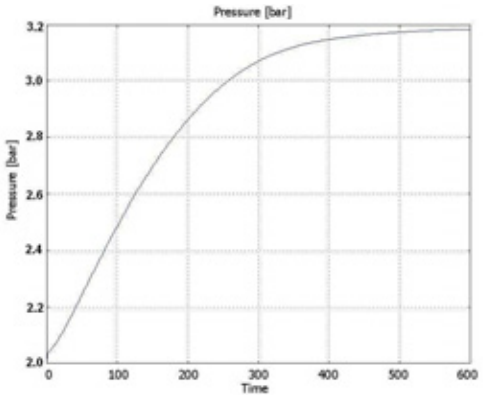

Figure 7. Internal pressure during desorption

5.2. Reactor 2

Our model has been validated for the simple geometry of the reactor 1 by comparing theoretical results and experimental data obtained from laboratory. After doing this, our model has been applied to a more complicated geometry in order to determine the thermal behaviour of a second reactor (reactor 2).

During absorption the temperature inside the reactor 2 (with fins) increases, showing the same behaviour as reactor 1 (without fins). The temperature in the vessel (figure 8) reaches its maximum value of about 24 °C, slightly lower than reactor 1. By a comparison of the various sketches of figure 9, higher temperature values are observable in the internal zone with respect to those close to walls, due to the external cooling bath at a constant temperature of 20 °C.

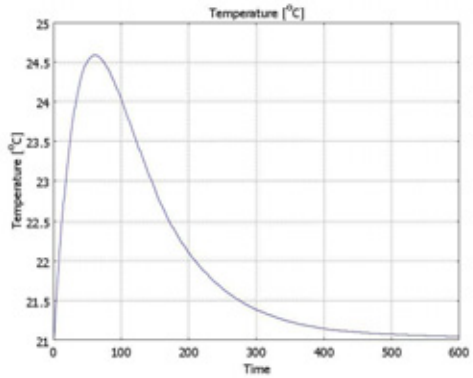

Figure 8. Temperature behaviour in the vessel 2 during absorption.

In desorption we observe a gradual increase in temperature from the initial value of 27 °C to the final value of about 40 °C corrisponding to the thermal equilibrium with the external bath. In the middle of the vessel (figure 10) the temperature increases because of the external heating; at about 150 s the endothermic process of desorption begins, leading to a decrease of the temperature. Finally, when the desorption has finished, the temperature rises again until the external fluid temperature is reached.

In figure 11 the evolution in time of the temperature of the reactor for the desorption case is showed.

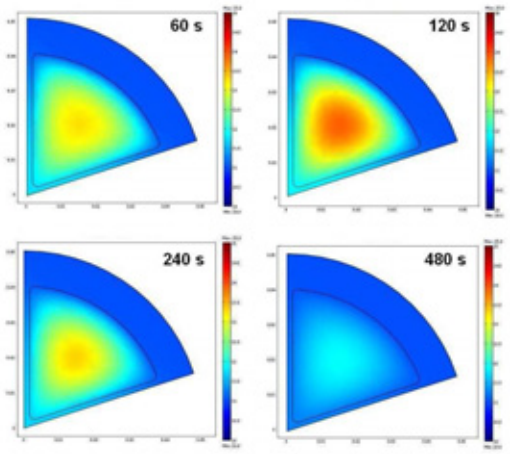

Figure 9. Time evolution of the vessel temperature (°C) at various times during absorption (60, 120, 240, 480 seconds).

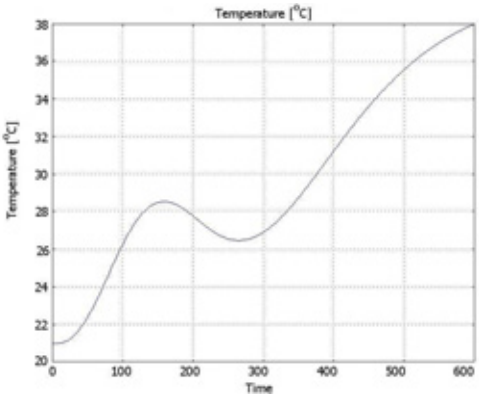

Figure 10. Temperature behaviour in the vessel 2 during desorption.

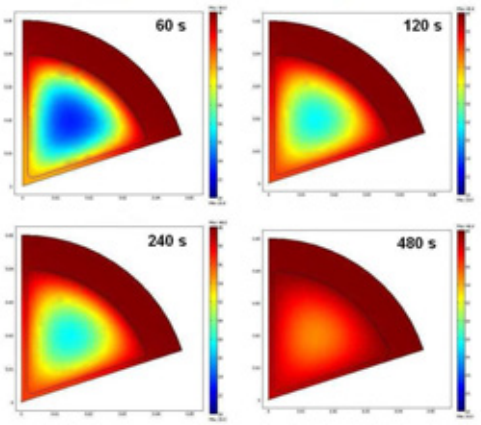

Figure 11. Time evolution of the vessel temperature (°C) at various times during desorption (60, 120, 240, 480 seconds).

5.3. Heat transfer parameters

The heat exchange in the system is correlated to two parameters: the effective thermal conductivity k_e (internal phenomena) and overall heat transfer coefficient h (external phenomena).

In order to evaluate the optimal heat transfer parameters, several numerical simulations were performed. In these simulations all the operative parameters were kept constant, except k_e and h, which have been allowed to vary.

The numerical results obtained were compared with experimental data in order to minimizing the error.

For thermal conductivity the best value founded was about 1.32 W m^{-1} K^{-1}, both for absorption and desorption simulations. Using this value as a constant, overall heat transfer coefficient was determinated too. The best h values founded are about 400 W m^{-2} K^{-1} for absorption and about 1000 W m^{-2} K^{-1} for desorption. The difference between the two cases are due to different external conditions.

6. Conclusions

In this work a model for a vessel containing a $LaNi_{4.8}Al_{0.2}$ hydride-based hydrogen storage tank has been presented.

Comparing the results obtained for reactors 1 and 2 (figure 12) it can be observed that the temperatures reached by the system are higher for the geometry without fins with respect to the geometry with fins (30 °C instead of 24 °C).

The theoretical results regarding the reactor 1 presented in this paper are in good agreement with experimental data. Optimal values for the heat transfer parameters k_e and h were established for both cases.

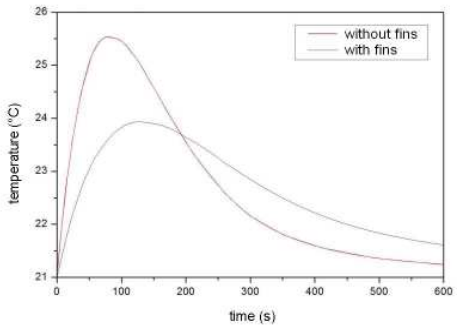

Figure 12. Comparison of the theoretical temperature inside the vessel during absorption between reactor 1 (without fins) and reactor 2 (with fins)

7. References

[1] K. Aldas, M.D. Mat, Y. Kaplan, A three-dimensional mathematical model for absorption in a metal hydride bed, *Int J Hydrogen Energy*, **27**, 1049-1056 (2002)

[2] S.B. Nasrallah, A. Jemni, Heat and mass transfer model in metal-hydrogen reactor, *Int J Hydrogen Energy*, **22**, 67-76 (1997)

[3] A. Jemni, S.B. Nasrallah, Study of two-dimensional heat and mass transfer during absorption in a metal-hydrogen reactor, *Int J Hydrogen Energy*, **20**, 43-52 (1995)

[4] A. Jemni, S.B. Nasrallah, Study of two-dimensional heat and mass transfer during desorption in a metal-hydrogen reactor, *Int J Hydrogen Energy*, **20**, 881-891 (1995)

[5] P. Marty, J.-F. Fourmigue, P. De Rango, D. Fruchart, J. Charbonnier, Numerical simulation of heat and mass transfer during the absorption of hydrogen in a magnesium hydride, *Energy Conversion and Management*, **47**, 3632-3643 (2006)

[6] C.A. Chung, C.-J. Ho, Thermal-fluid behaviour of the hydriding and dehydriding processes in a metal hydride hydrogen storage

canister, *Int J Hydrogen Energy*, **34**, 4351-4364 (2009)
[7] F. Laurencelle, Z. Dehouche, J. Goyette, T.K. Bose, Integrated electrolyser-metal hydride compression system, *Int J Hydrogen Energy*, **31**, 762-768 (2006)
[8] S. Mellouli, F. Askri, H. Dhaou, A. Jemni, S.B. Nasrallah, A novel design of heat exchanger for a metal-hydrogen reactor, *Int J Hydrogen Energy*, **32**, 3501-3507 (2007)
[9] M.Y. Ha, I.K. Kim, H.D. Song, S.Sung, D.H. Lee, A numerical study of thermo-fluid phenomena in metal hydride beds in the hydriding process, *Int J Heat Mass Transfer*, **47**, 2901-2912 (2004)

8. Acknowledgements

The experimental support of Dr. Salvatore Galliano of HysyLab, Environment Park, Torino (Italy) is gratefully acknowledged.

9. Nomenclature

C	Kinetic constant [s^{-1}]
C_p	Specific heat [J kg^{-1} K^{-1}]
E	Activation energy [J mol^{-1}]
h	Overall heat transfer coefficient [W m^{-2} K^{-1}]
K	Permeability [m^2]
k	Thermal conductivity [W m^{-1} K^{-1}]
m	Source term [kg m^{-3} s-^{1}]
M	Molecular weight [kg mol^{-1}]
p	Pressure [Pa]
R_g	Universal gas constant [J mol^{-1} K^{-1}]
T	Temperature [K]
t	Time [s]
v	Gas velocity [m s^{-1}]

Greek symbols:

ΔH	Enthalpy [J mol^{-1}]
ΔS	Entropy [J mol^{-1} K^{-1}]
ε	Porosity [-]
μ	Dynamic viscosity [kg m^{-1} s^{-1}]
ρ	Density [kg m^{-3}]

Subscripts:

a	Absorption
d	Desorption
e	Effective
eq	Equilibrium
f	External fluid
g	Gas
s	Hydride
ss	Saturation
0	Initial